



TITLE:

Structure of Fe-C Multilayered Films (Commemoration Issue Dedicated to Professor Toshio TAKADA On the Occasion of His Retirement)

AUTHOR(S):

Nakayama, Noriaki; Katamoto, Tsutomu; Shinjo,
Teruya; Takada, Toshio

CITATION:

Nakayama, Noriaki ...[et al]. Structure of Fe-C Multilayered Films (Commemoration Issue Dedicated to Professor Toshio TAKADA On the Occasion of His Retirement). Bulletin of the Institute for Chemical Research, Kyoto University 1986, 64(4): 170-180

ISSUE DATE:

1986-12-06

URL:

<http://hdl.handle.net/2433/77163>

RIGHT:

Structure of Fe-C Multilayered Films

Noriaki NAKAYAMA*, Tsutomu KATAMOTO*^{**,} Teruya SHINJO*
and Toshio TAKADA*

Received May 16, 1986

Multilayered films composed of very thin iron and carbon layers were prepared and their structures were investigated from X-ray diffraction and electron microscopy. Fe layers have a bcc structure when their thickness is 30 Å, whereas amorphous like structure when 15 Å and 8 Å. On the other hand, carbon layers are always amorphous. The results of X-ray diffraction are satisfactorily simulated by calculated patterns, indicating the flatness of each interface.

KEY WORDS: Fe-C multilayered films/ X-ray diffraction/ Electron microscopy/

1. INTRODUCTION

Multilayered films with artificial superstructure (Artificial superstructure film: ASF) have attracted much attention as a new class of material.¹⁾ In our laboratory, many ASF's composed of a ferromagnetic metal (Fe or Co) and a nonmagnetic metal (Sb, V, Mg etc.) have been investigated.²⁾ The main aim of their investigations is to study the interface magnetism or the magnetic properties of ultra-thin ferromagnetic films.

The combination of iron and carbon is especially interesting from the following viewpoints.

1) Evaporated carbon films are known to have amorphous structure and to be very flat even when their thicknesses are less than 100 Å. They have long been used in the sample preparation for the electron microscopic observations.³⁾ Thus, carbon films will be very good supporting materials of ultra-thin metal films.

2) X-ray and electron atomic scattering factors of carbon atoms are much smaller than those of Fe atoms. Therefore, the structural characterization of multilayered films is relatively easy.

3) ASF's composed of a large atomic number element (such as W or Au) and carbon have been investigated by many researchers as X-ray monochrometers or X-ray mirrors in the field of the synchrotron radiation usage or X-ray microscopy.^{4,5)} It has been pointed out in these studies that amorphous metal layers have flat structures.⁶⁾ Also, the enhancement of X-ray reflectivity by thermal annealing of sample was reported.⁵⁾ The carbide formation at the metal-carbon interface should play an important role. The Fe-C ASF is a good system to investigate the carbide formation at the metal-carbon interface.

* 中山則昭, 片元 勉, 新庄輝也, 高田利夫: Laboratory of Solid State Chemistry, Institute for Chemical Research, Kyoto University, Uji, Kyoto-fu 611.

** Present address: Toda-Kogyo Co. Ltd., Naka-ku, Hiroshima 733.

In this paper, we describe the preliminary results of sample preparation and structural characterization of Fe-C multilayered films.

2. EXPERIMENTAL

Samples are prepared by the alternate vacuum deposition of Fe and C in the ultra-high vacuum. The base pressure of the vacuum system is 10^{-9} Torr. Source materials are iron ingot and pressed pyrolytic graphite. They are evaporated by an electron beam heating system. The pressure during the evaporation is in the order of 10^{-8} Torr. The thickness of deposited layer and the deposition rate are measured by a quartz oscillator thickness monitor. The typical deposition rate of Fe layer was 0.2 \AA/sec . The substrate was kept at -20°C during the deposition of Fe layers. In the case of carbon layer deposition, the substrate temperature is raised up to around 100°C due to the thermal radiation. The sensor for the thickness monitor also is heated up and the thickness determination becomes inaccurate. After closing the shutter and waiting for a while until the temperature returns to the room temperature, the nominal thickness of carbon layers is estimated. Accordingly the thickness of each carbon layers is not constant but fluctuates to some extent. The substrate materials are glass plates, mylar films, Kapton polyimide films and tri-acetyle cellulose (TAC) films. The layer thicknesses of several samples are listed in Table I.

Samples are characterized by the X-ray diffraction and electron microscopy. X-ray diffraction experiments are performed using a conventional diffractometer equipped with a diffracted beam monochromator of pyrolytic graphite. The X-ray used for the measurements is $\text{Cu-K}\alpha$ radiation from a rotating anode type X-ray generator (RIGAKU-RU200). Diffraction patterns are obtained by setting the scattering vector perpendicular to the film plane and by the θ - 2θ scan method. Electron diffraction patterns and electron micrographs are obtained using a JEM-100CX electron microscope. Samples for electron microscopic observations are those deposited on TAC films. The substrate TAC film is dissolved into ethyl-acetate. Then, fragments of Fe-C multilayered films are collected on copper meshes.

Table I Thickness of individual Fe (D_{Fe}) and C (D_{C}) layers in the prepared Fe-C multilayered films. D_{Fe} and D_{C} were measured by quartz oscillator thickness monitor.

sample	number of Fe layers	D_{Fe} (Å)	average D_{C} (Å)	D_{C} in the order of deposition (Å)
I	4	104*	101	104-99-101-99-100
II	15	30	99	95-141-104-88-89-89-113-95-95-93-95-94-93-104-91-111
III	24	15	40	70-39-39-38-57-46-39-38-39-45-38-41-41-43-40-41-42-41-50-39-34-41-38-39-32
IV	25	8	61	99-53-55-55-57-64-60-57-54-52-51-60-53-57-56-60-55-53-53-70-57-60-59-59-64-53

* ^{56}Fe 100Å + ^{57}Fe 4Å; deposition order is ^{56}Fe - ^{57}Fe -C

3. RESULTS AND DISCUSSION

X-ray diffraction patterns of prepared Fe-C multilayered films show sharp diffraction peaks in the small angle region. The appearance of these peaks indicates both Fe and C layers being reasonably flat. Figure 1(a) shows the diffraction pattern of sample I. The individual Fe layer thicknesses are all 104Å. The individual C layer thicknesses measured by thickness monitor are 104Å, 99Å, 101Å, 99Å and 100Å. Only four bilayers give such sharp peaks in the X-ray diffraction pattern although some splitting due to the fluctuation of carbon layer thickness is recognized in the lower order peaks. The artificial periodicity calculated by the peak angle θ_1 and θ_2 of two successive peaks using the formula

$$1/\Lambda = 2 \sin \theta_1/\lambda - 2 \sin \theta_2/\lambda$$

(λ : X-ray wave length)

is 105Å. This is the half of the multilayer periodicity, which is caused by the extinction condition due to the nearly equal layer thickness of Fe and C layers. Namely,

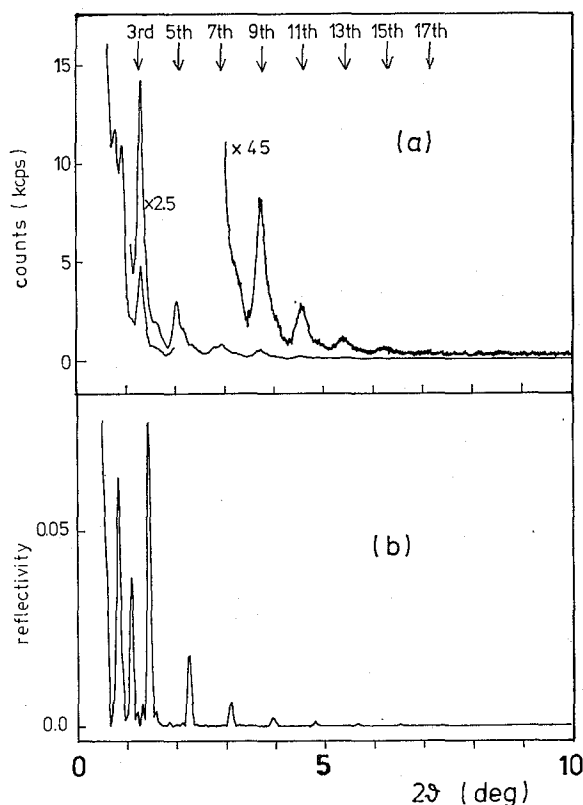


Fig. 1. X-ray diffraction patterns in the small angle region of sample I. (a) Observed profile of sample deposited on glass substrate. Arrows indicate the peak positions expected from the artificial periodicity of 210 Å. (b) Simulated profiles for this multilayer by Underwood and Barbee's method.

the even order peaks disappear as were indexed in the figure. To confirm the extinction condition, the X-ray reflectivity of this multilayer was simulated using the method by Barbee and Underwood.⁷⁾ The results are shown in Fig. 1(b). The calculated profile of X-ray reflectivity as a function of grancing angle quite well agrees with the observed diffraction pattern. The average periodicity of this multi-

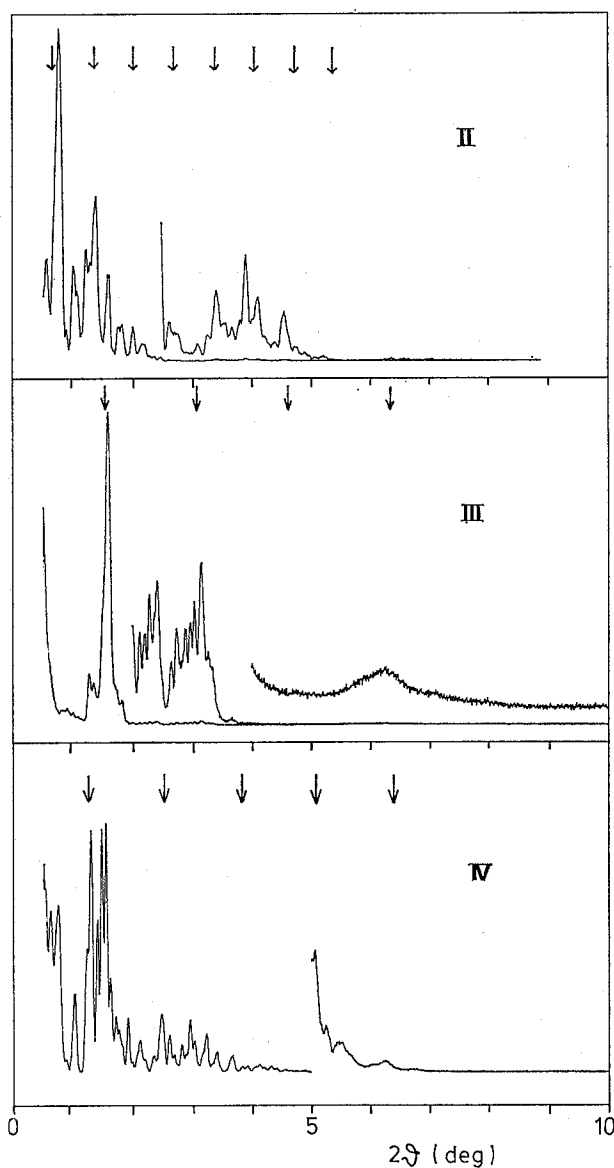


Fig. 2. Observed X-ray diffraction profiles of sample II ($D_{\text{Fe}}=30$ Å), III ($D_{\text{Fe}}=15$ Å) and IV ($D_{\text{Fe}}=8$ Å) deposited on glass substrates. Bragg peak positions expected for the Fe-C ASF with constant carbon layer thicknesses (equal to the average D_{C} in Table 1) are marked by arrows.

layer is estimated as 210\AA , which is nearly the same as the design value by thickness monitor. The appearance of sharp peaks in the diffraction pattern indicates the flatness of both Fe and C layers. The intense diffraction peak is originated from the large difference in the X-ray scattering powers between Fe and C layers.

X-ray diffraction patterns of sample II, III and IV deposited on glass substrates are shown in Fig. 2. In these samples, carbon layer thicknesses fluctuated to a certain extent. Many peaks appear in these diffraction patterns but they have strong intensities near the ideal Bragg peak positions expected for the ideal ASF with a constant carbon layer thickness. Ideal Bragg peak positions are marked in the figure. Especially, the diffraction pattern of sample III with $D_{\text{Fe}}=15\text{\AA}$, in which the deviation of individual carbon layer thicknesses from average value is small, shows fairly sharp peaks at the ideal positions. The simulated profile in Fig. 3 by Underwood & Barbee's method reproduces the observed profile fairly well. The higher order peaks are rather broad due to the fluctuation of periodicity. The similar broadening of diffraction peaks was reported in the case of Fe-Mg ASF.⁸⁾ The periodicity calculated from peak position of observed 4th order reflection is 58\AA , which is in agreement with the thickness measured by the quartz oscillator. It is notable that the fine structure of lower order reflection is caused by the flatness of Fe-C multilayers. It represents the ripple in the X-ray reflectivity due to the total layer thickness of the film. Above observations are all on the samples deposited on glass substrates. In the case of samples deposited on Kapton films, fairly sharp peaks without ripple are observed as shown in Fig. 4. Because of the microscopic roughness of substrate, the ripples are smeared out.

In the higher angle region of X-ray diffraction pattern, no sharp diffraction peaks are observed. A broad peak appears only near the peak position of (110) reflection of bulk bcc-Fe as shown in Fig. 5. The absence of other diffraction peaks

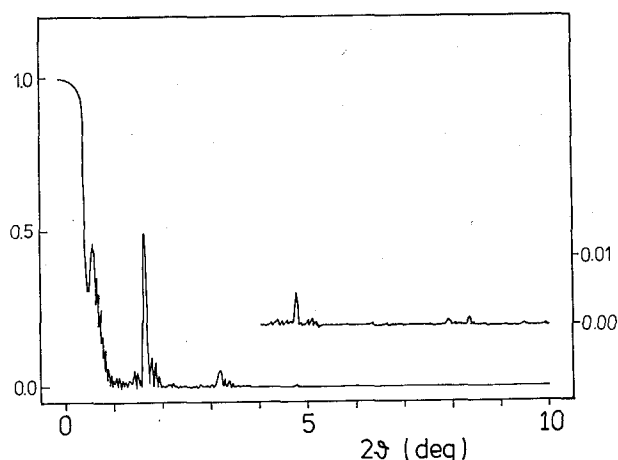


Fig. 3. Simulated profile of Fe-C multilayer in which Fe and C layers have same thicknesses with those in sample III measured by thickness monitor. The calculation was performed by Underwood and Barbee's method.

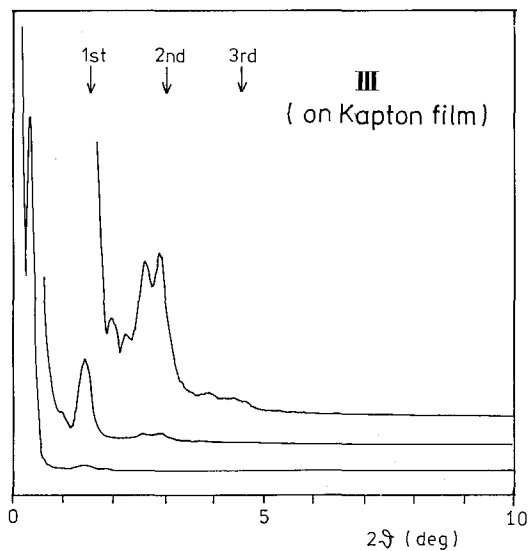


Fig. 4. Observed profile of sample III ($D_{\text{Fe}}=15 \text{ \AA}$) deposited on Kapton film. Arrows indicate peak positions of ideal ASF with $D_{\text{Fe}}=15 \text{ \AA}$ and $D_{\text{C}}=40 \text{ \AA}$.

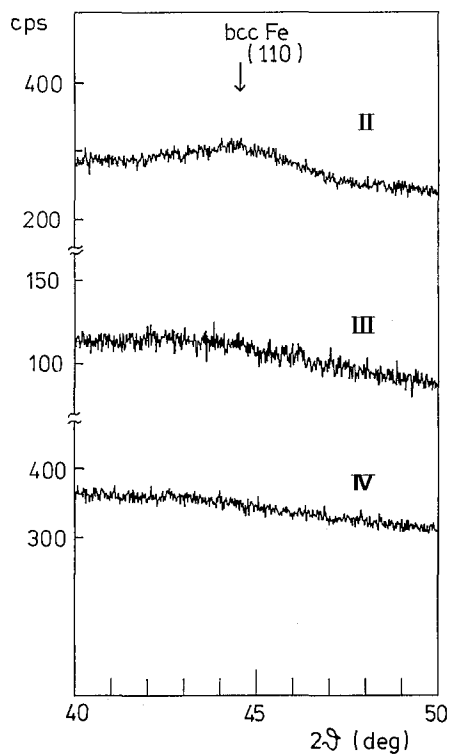


Fig. 5. X-ray diffraction profiles in the higher angle region of sample II ($D_{\text{Fe}}=30 \text{ \AA}$), III ($D_{\text{Fe}}=15 \text{ \AA}$), and IV ($D_{\text{Fe}}=8 \text{ \AA}$) deposited on glass substrates.

indicates that carbon layers are amorphous. In the case of sample II with individual Fe layer thickness of 30\AA , the peak position is close to that of bcc-Fe (110) peak. The full width at half maximum (FWHM) of this peak corresponding to the particle size along film normal of 30\AA following to the Scherrer's formula. This value corresponds to the individual Fe layer thickness, which is typical for the amorphous-crystalline ASF's as pointed in the case of Co-Sb multilayered films and is due to the fluctuation in thicknesses of amorphous layers.⁹⁾ The thinner the individual Fe layer thickness, the broader the FWHM and the smaller the peak angle.

Figure 6 shows the electron diffraction patterns of Fe-C multilayered films.

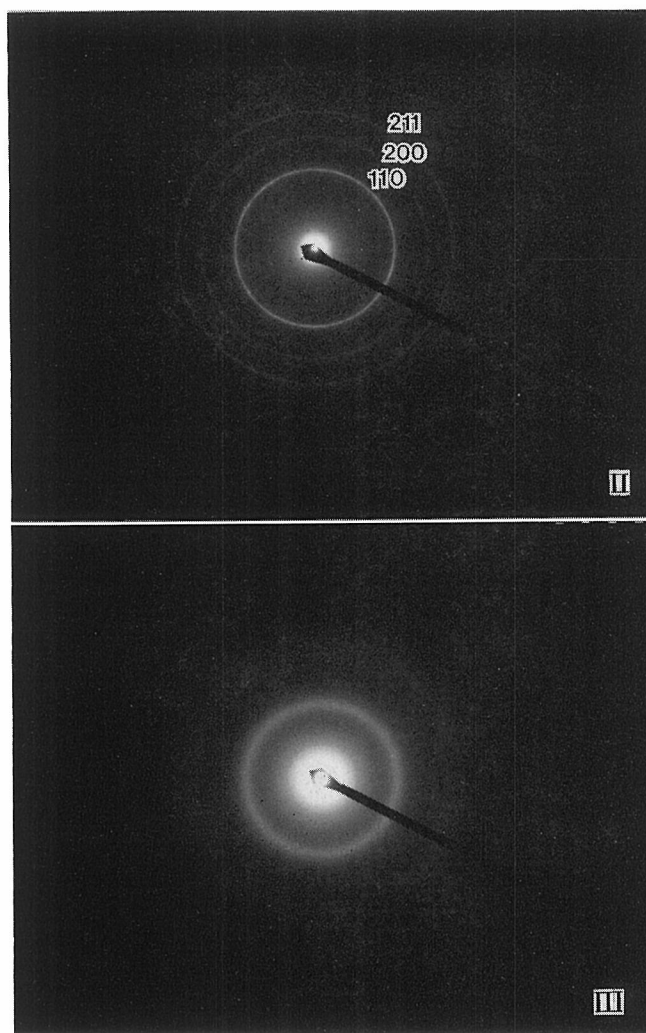


Fig. 6. Electron diffraction pattern of sample II ($D_{\text{Fe}}=30\text{\AA}$) and III ($D_{\text{Fe}}=15\text{\AA}$). Sample IV ($D_{\text{Fe}}=8\text{\AA}$) shows similar diffraction pattern with sample III. Electron beam incidence is perpendicular to the film plane. Note the broad diffraction ring in the case of sample III.

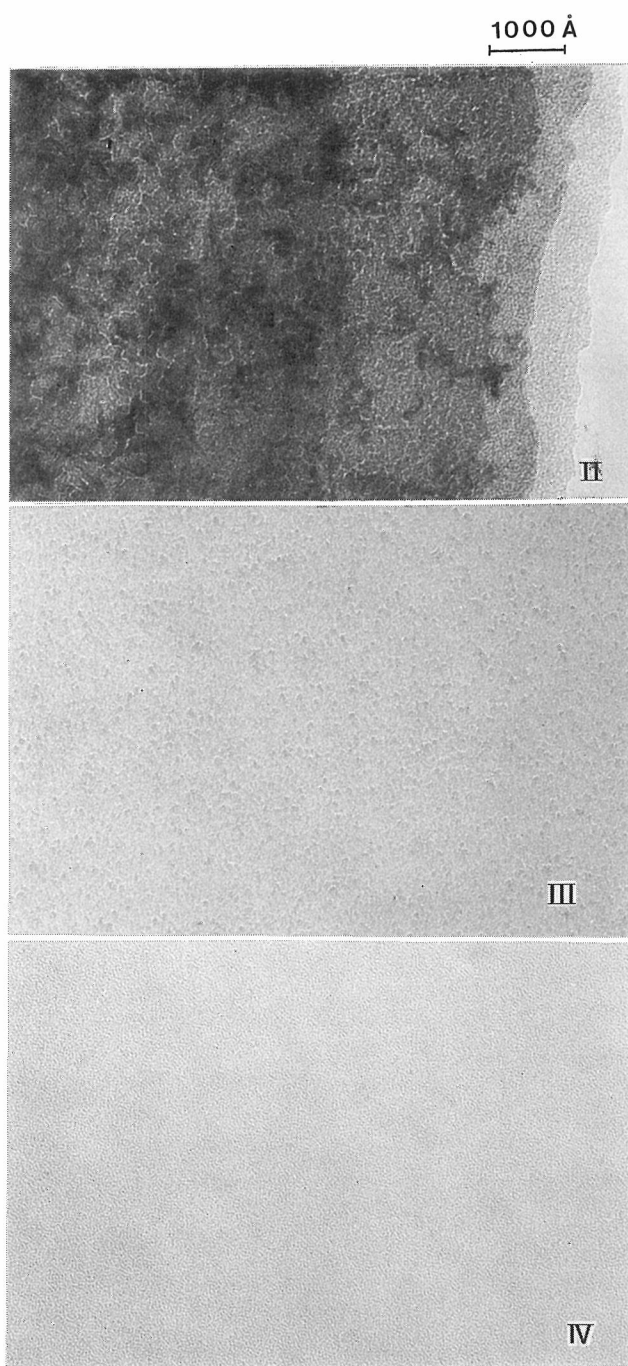


Fig. 7. Bright field image of sample II, III and IV. Note the difference in the crystallinity.

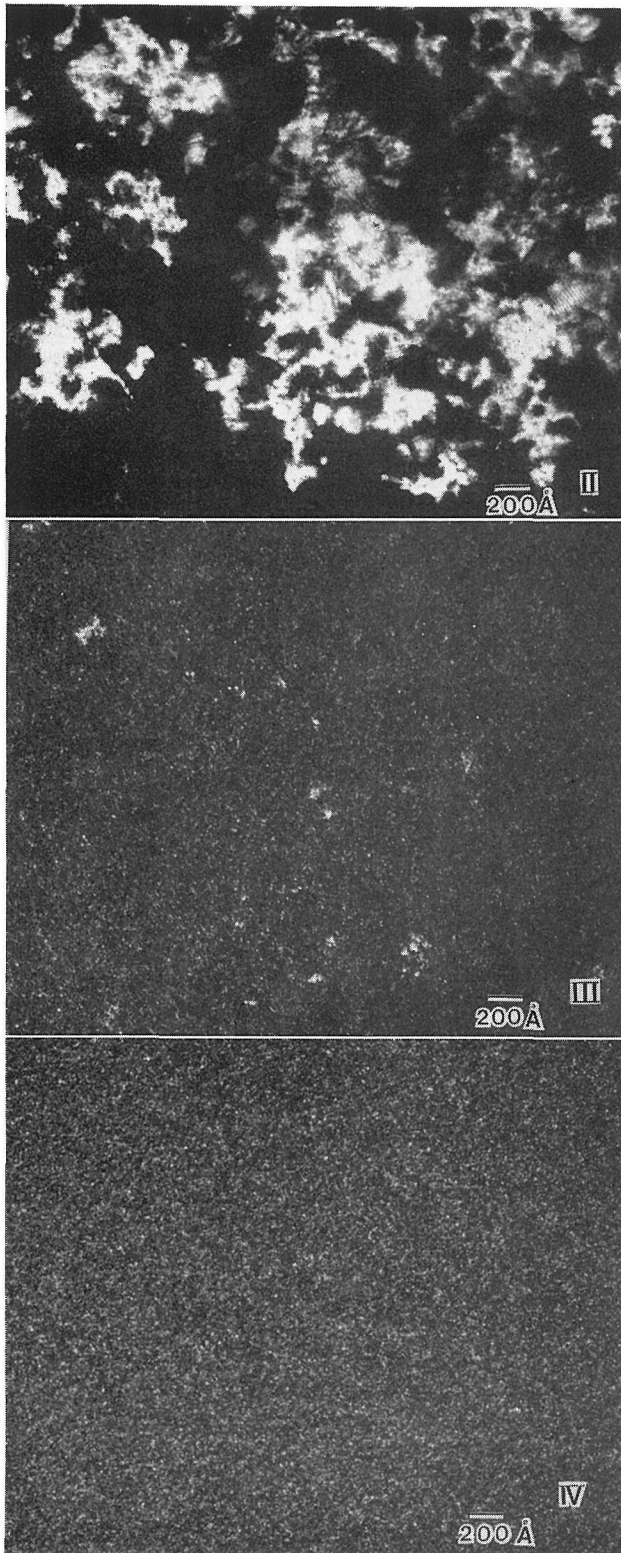


Fig. 8. Dark field images of sample II, III and IV. A small objective aperture was located on bcc-Fe (110) diffraction ring or the corresponding one for imaging.

Their electron beam incidence is perpendicular to the film plane. The diffraction patterns of sample I ($D_{\text{Fe}}=104\text{\AA}$) and II ($D_{\text{Fe}}=30\text{\AA}$) show sharp diffraction rings which can be indexed as those of bcc-Fe. However, those of sample III ($D_{\text{Fe}}=15\text{\AA}$) and IV ($D_{\text{Fe}}=8\text{\AA}$) show only very broad diffraction rings near the (110) and (211) reflection of bcc-Fe. In both types of electron diffraction pattern, diffraction ring from carbon layers cannot be observed similarly to X-ray diffraction patterns in the higher angle region. This also evidences the amorphous structure of carbon layers. The bright field images also show a significant change as the individual Fe layer thicknesses decrease. Sample II shows a high contrast image, which indicates that Fe layers are crystalline. Sample III and IV show low contrast images which are typical for the amorphous structure. The grains of bcc-Fe particles can not be distinguished. Dark field images (DFI) of these samples shown in Fig. 8 also reveal the difference of the structure. For imaging, a small objective aperture was located on the bcc-Fe (110) diffraction ring or the corresponding broad ring in cases of sample III and IV. The DFI of sample II resolves bcc-Fe particles with mean inplane size of about 100\AA . In some parts the moiré fringes can be seen. The moiré fringe seems to be originated from the crystallographic axis being rotated between adjacent Fe layers. The DFI of sample III and IV only shows ultra-fine white dots, which are typical for an amorphous structure. DFI of sample III shows the contrast indicating the very small crystalline particles in some places.

These X-ray diffraction experiments and electron microscopic observations indicate that Fe layers in sample III and IV have an amorphous like structure. This is also indicated by the Mössbauer experiments. The spectrum of sample II with $D_{\text{Fe}}=30\text{\AA}$ shows a sharp six-line magnetic splitting which indicates the bcc structure of Fe layers in this sample. The spectra of sample III and IV also show magnetic splitting. However, the magnetic hyperfine fields are much smaller than bcc-Fe and fairly distributed. The average magnetic hyperfine field at room temperature was estimated by a histogram method to be 190 kOe for sample III and 50 kOe for sample IV. The detailed analysis of ^{57}Fe Mossbauer spectra will be described elsewhere. This result is similar to those on amorphous Fe-C alloys. The reduction of the hyperfine field suggests that Fe layers include some amount of C.

4. SUMMARY

Nearly periodic multilayered films of Fe and C were prepared. Carbon layers have amorphous structure. Fe layers have bcc structure when Fe layer thickness is 30Å and 104Å. When Fe layer thickness is 15Å and 8Å, iron layers are amorphous probably due to the carbide formation. Such a structural change of thin Fe layers by their thickness is also reported in the case of Fe-Mg ASF's recently investigated in this laboratory.^{8),10)}

Fe-C multilayered films are appropriate model substances to investigate the magnetic properties of ultra-thin ferromagnetic films with amorphous structure, as is predicted by Chudonovsky.¹¹⁾ The flatness of amorphous carbon layers is the most attractive point in the sample preparation. High quality ASF's with Fe layers even

less than 8Å will be obtained if the carbon layer thicknesses are precisely controlled and a flat substrate is used.

REFERENCES

- (1) See a review, 'Synthetic Modulated Structures', L. Chang and B.C. Giessen Eds. (Academic Press, New York, 1985)
- (2) T. Shinjo, N. Hosoi, K. Kawaguchi, T. Takada, Y. Endoh, Y. Ajiro and J.M. Friedt, *J. Phys. Soc. Japan.*, **52**, 3154 (1983); T. Shinjo, N. Hosoi, K. Kawaguchi, N. Nakayama, T. Takada and Y. Endoh, *J. Magn. Magn. Mat.*, **54-57**, 54 (1986); references there in.
- (3) A. Fukami, K. Adachi and M. Katoh, *J. Electron Microscopy*, **21**, 99 (1972)
- (4) T.W. Barbee, Jr., AIP Conf. Proc. **75**, 131 (1981)
- (5) T.W. Barbee, Jr., in 'X-ray Optics', eds. G. Schmahl and D. Rudolph, (Springer-Verlag, Berlin Heidelberg, 1984) p. 144
- (6) R.P. Haelbich, A. Segmuller and E. Spiller, *Appl. Phys. Lett.*, **34**, 184 (1979)
- (7) J.H. Underwood and T.W. Barbee, Jr., *Appl. Optics*, **20**, 3027 (1981)
- (8) Y. Fujii, T. Ohnishi, T. Ishihara, Y. Yamada, K. Kawaguchi, N. Nakayama and T. Shinjo, *J. Phys. Soc. Japan.*, **55**, 251 (1986)
- (9) N. Nakayama, K. Takahashi, T. Shinjo, T. Takada and H. Ichinose, *Japn. J. Appl. Phys.*, **25**, 552 (1986)
- (10) T. Shinjo, K. Kawaguchi, R. Yamamoto, N. Hosoi and T. Takada, *Solid State Comm.*, **52**, 257 (1984); K. Kawaguchi, R. Yamamoto, N. Hosoi, T. Shinjo and T. Takada, *J. Phys. Soc. Jap.*, **55**, 2375 (1986).
- (11) M. Chudonovsky, *J. Magn. Magn. Mat.*, **40**, 21 (1983)